

# Determination of lipidomic differences between human breast cancer and surrounding normal tissues using HILIC-HPLC/ESI-MS and multivariate data analysis

Eva Cífková · Michal Holčápek · Miroslav Lísa · David Vrána · Jiří Gatěk · Bohuslav Melichar

Received: 15 June 2014 / Revised: 10 September 2014 / Accepted: 14 October 2014 / Published online: 29 October 2014  
© Springer-Verlag Berlin Heidelberg 2014

**Abstract** The comprehensive approach for the lipidomic characterization of human breast cancer and surrounding normal tissues is based on hydrophilic interaction liquid chromatography (HILIC)–electrospray ionization mass spectrometry (ESI-MS) quantitation of polar lipid classes of total lipid extracts followed by multivariate data analysis using unsupervised principal component analysis (PCA) and supervised orthogonal partial least square (OPLS). This analytical methodology is applied for the detailed lipidomic characterization of ten patients with the goal to find the statistically relevant differences between tumor and normal tissues. This strategy is selected for better visualization of differences, because the breast cancer tissue is compared with the surrounding healthy tissue of the same patient, therefore changes in the lipidome are caused predominantly by the tumor growth. A large increase of total concentrations for several lipid classes is observed, including phosphatidylinositols, phosphatidylethanolamines, phosphatidylcholines, and lysophosphatidylcholines. Concentrations of individual lipid species inside the abovementioned classes are also changed, and in some cases,

these differences are statistically significant. PCA and OPLS analyses enable a clear differentiation of tumor and normal tissues based on changes of their lipidome. A notable decrease of relative abundances of ether and vinyl ether (plasmalogen) lipid species is detected for phosphatidylethanolamines, but no difference is apparent for phosphatidylcholines.

**Keywords** Breast cancer · Lipid biomarkers · HILIC-HPLC/ESI-MS · Quantitation · Statistical analysis

## Introduction

Breast cancer is the most common malignant tumor in women population and one of the most common causes of death from cancer [1, 2]. Breast cancer represents a group of different neoplastic disorders originating in the same organ rather than a single disease entity. At least four breast cancer subtypes with distinct biology and clinical presentation are currently recognized, including two subtypes characterized by the expression of hormone receptors (luminal A tumors and luminal B tumors), human epidermal growth factor (HER)-2 positive, and triple negative breast cancer. While tissue diagnosis is based on the histological evaluation of the tumor tissue, there is still an unmet medical need for biomarkers that would reliably reflect the disease burden.

Lipids are the building blocks of cell membranes, and the lipidomic composition can change during the malignant transformation. Lipid metabolism plays an important role in oxidative stress and is associated, among other parameters, with factors linked to the breast cancer risk including hormonal balance, body mass index, breast density, drug metabolism, and growth of insulin levels [3]. The potential effect of fat diet and changes of lipid metabolism on cancer progression and aggressiveness of cancer cells has been suggested by several lipidomic studies that compare fatty acid composition in tumor vs. normal tissues [4, 5] or blood of breast cancer patients

Published in the topical collection celebrating *ABCs 13th Anniversary*.

**Electronic supplementary material** The online version of this article (doi:10.1007/s00216-014-8272-z) contains supplementary material, which is available to authorized users.

E. Cífková · M. Holčápek (✉) · M. Lísa  
Department of Analytical Chemistry, Faculty of Chemical  
Technology, University of Pardubice, Studentská 573,  
532 10 Pardubice, Czech Republic  
e-mail: Michal.Holcapek@upce.cz

D. Vrána · B. Melichar  
Department of Oncology, Medical School and Teaching Hospital,  
Palacký University, I.P. Pavlova 6, 775 20 Olomouc, Czech Republic

J. Gatěk  
Department of Surgery, Atlas Hospital, Tomáš Baťa University in  
Zlín, nám. T.G. Masaryka 5555, 760 01 Zlín, Czech Republic

vs. healthy controls [6, 7] using gas chromatography (GC) coupled with flame ionization detection (FID) or mass spectrometry (MS). Several studies [4–6, 8, 9] report the ratio of *n*-6 polyunsaturated fatty acids (PUFA) to *n*-3 PUFA being a key factor for tumor angiogenesis that is essential for tumor growth and metastasis. The major *n*-6 PUFA is linoleic acid (FA 18:2), which can be metabolized into arachidonic acid (FA 20:4). *n*-3 PUFA are represented mainly by  $\alpha$ -linolenic acid (FA 18:3), docosahexaenoic acid (FA 22:6), and eicosapentaenoic acid (FA 20:5). In past, the ratio of *n*-6/*n*-3 PUFA was close to 1:1, but the current Western diet has resulted in the change of this ratio up to 15:1 [8, 10], which is considered as a potential risk factor for many disorders including cancer.

Various lipidomic approaches have been used for the analysis of phospholipid composition in breast cancer cell lines [11–14], human tumor and normal tissues [15, 16], or human body fluids (blood or urine) [17, 18]. Reports on the differences of phospholipid composition between mammary epithelial cells and breast cancer cells with different biological behaviors show rather conflicting results mainly for phosphatidylethanolamines (PE), lysophosphatidylcholines (LPC), and cardiolipins in different cancer cells [11, 12]. In another study, total concentrations of phosphatidylcholines (PC) and PE are increased by more than 41 % in breast cancer patients compared with healthy controls [18].

The coupling of high-performance liquid chromatography and mass spectrometry (HPLC/MS) is the technique most frequently used for highly sensitive and selective lipidomic characterization with the possibility to identify and quantify complex mixtures of polar and nonpolar lipids, relatively rapid screening of various biological samples [19]. Reversed-phase HPLC makes possible to separate individual lipid species differing in fatty acyl chain lengths and the number of double bonds, while hydrophilic interaction liquid chromatography (HILIC) is more convenient for the separation of lipid classes. MS coupled with the direct infusion (shotgun approach) is the technique commonly used for rapid lipidomic analyses using product ion, neutral loss, and the selected reaction monitoring scans typical for triple quadrupoles (QqQ) and other hybrid tandem mass analyzers [20, 21].

Magnetic resonance imaging (MRI) [22–25] is used for the noninvasive *in vivo* characterization of breast tissues that can improve the specificity of tumor diagnostics, monitoring of tumor responses to systemic treatment, and analyses of tumor tissues *in vivo* and *in vitro* [1]. H MRI and [31] P MRI are used for the monitoring of significant differences in phospholipid metabolites in normal and tumor breast tissues. Increased relative abundances are reported for choline metabolites and most phospholipid classes except for PC, LPC, plasmalogen phosphatidylethanolamines (pPE), and phosphatidylserines (PS) [25]. MRI is used mainly as a diagnostic tool in medicine due to low sensitivity and selectivity.

The main challenge in the lipidomic studies of biological samples is the evaluation of data sets of large size and complexity [26]. At present, principal component analysis (PCA) and techniques based on partial least square projections to latent structures (PLS) are often used for multivariate data analysis (MDA) in multiple omics platforms [27]. The principle of PCA is finding a transformation that reduces the dimensionality of the data by conversion of a set of correlated variables to a new set of uncorrelated variables called principal components [27]. PLS finds the linear correlations (predictive variables) between dependent variables (Y matrix) and predictor variables (X matrix). There is a risk that variations in X matrix are not linearly correlated with Y matrix in PLS [27, 28]. For this reason, orthogonal partial least square (OPLS) [27, 29] is enhanced, and the latent variables are divided into linearly correlated (predictive) and nonlinearly (orthogonal) correlated variables between X and Y matrices (variables in X orthogonal to Y). In contrast to unidirectional correlations of PLS and OPLS (i.e.,  $X \rightarrow Y$ ), orthogonal 2 projections to latent structures (O2PLS) [27, 30] is described using bidirectional correlations (i.e.,  $X \leftrightarrow Y$ ). Generally, latent variables in O2PLS are partitioned into predictive variables, variables in X orthogonal to Y and variables in Y orthogonal to X. Advantages of O2PLS in comparison to PLS are better data interpretability, clear selection of outliers, reduction of model complexity, determination the number of components, etc. [26, 27, 30].

This paper describes the application of our previously reported quantitative approach for the lipidomic characterization of changes in breast cancer tissues compared with surrounding normal tissues using HILIC-HPLC/electrospray ionization mass spectrometry (ESI-MS). The lipid class quantitation by HILIC is used for the first time for the clinical study, and this approach clearly shows differences in lipidomes of tumor and normal tissues. Observed differences in the lipidome caused by the tumor growth are visualized by both unsupervised and supervised MDA.

## Experimental

### Chemicals and standards

Acetonitrile, 2-propanol, methanol (all HPLC/MS grade), chloroform stabilized by 0.5–1 % ethanol and hexane (both HPLC grade), and ammonium acetate were purchased from Sigma-Aldrich (St. Louis, MO, USA). Deionized water was prepared with a Demiwa 5-roi purification system (Watek, Ledeč nad Sázavou, Czech Republic). *N*-Dodecanoyl-heptadecasping-4-enine-1-phosphoethanolamine (d17:1/12:0) used as an internal standard (IS) for the nontargeted quantitation was purchased from Avanti Polar Lipids (Alabaster, AL, USA). Human breast tumor and surrounding normal

tissues of ten patients (see Electronic Supplementary Material (ESM) Table S1) were obtained from the Department of Surgery, Atlas Hospital Zlín in the Czech Republic. All patients have read and signed the informed consent approved by the Hospital Ethical Committee. No sample was excluded from the statistical evaluation.

### Sample preparation

Human breast tumor tissues and surrounding normal tissues were extracted according to a modified Folch procedure [31] using a chloroform–methanol–water system. Briefly, 50–150 mg of human tissue and 25  $\mu$ L of 3.3 mg/mL IS were homogenized with a 5-mL mixture of chloroform–methanol (2:1, v/v), and the homogenate was filtered using a coarse filter paper. Subsequently, 1 mL of 1 mol/L NaCl was added, and the mixture was centrifuged at 3000 rpm for 5 min at room temperature. The chloroform bottom layer (total lipid extract) containing the lipids was evaporated by a gentle stream of nitrogen and redissolved in chloroform–2-propanol mixture (1:1, v/v) for HILIC-HPLC/MS analyses. Total lipid extracts were purified using re-extraction with hexane–methanol–water system to remove the excess of nonpolar lipids, mainly triacylglycerols (TG). Briefly, 100  $\mu$ L of total lipid extract was mixed with a 900- $\mu$ L mixture of hexane–methanol–water (4:1:1, v/v/v). The extract was divided into hexane (upper) layer containing mainly nonpolar lipids and methanol–water (bottom) layer containing mainly polar lipids. Polar lipid extracts were evaporated by a gentle stream of nitrogen and redissolved in chloroform–2-propanol mixture (1:1, v/v) for HILIC analyses.

### HILIC-HPLC/ESI-MS conditions

Lipidomic analyses were performed on a liquid chromatograph Agilent 1200 series (Agilent Technologies, Waldbronn, Germany) coupled with the Esquire 3000 ion trap analyzer (Bruker Daltonics, Bremen, Germany). Lipid extracts were separated into individual lipid classes using a Spherisorb Si column (250 $\times$ 4.6 mm, 5  $\mu$ m, Waters, Milford, MA, USA), a flow rate of 1 mL/min, an injection volume of 10  $\mu$ L, column temperature of 40  $^{\circ}$ C, and a mobile phase gradient: 0 min, 94 % A+6 % B and 60 min, 77 % A+23 % B, where A was acetonitrile and B was 5 mM aqueous ammonium acetate [32]. Individual lipid classes were detected in the positive- and negative-ion ESI modes in the mass range  $m/z$  50–1000 with the following setting of tuning parameters: pressure of the nebulizing gas, 60 psi; drying gas flow rate, 10 L/min; and temperature of the drying gas, 365  $^{\circ}$ C. The acquired data were quantified using the nontargeted lipidomic analysis of individual lipid classes using the single IS and response factors described earlier [33]. Individual lipids within phosphatidylinositol (PI) and PE classes were identified and

quantified using relative intensities of deprotonated molecules  $[M-H]^{-}$  and PC using relative intensities of  $[M-CH_3]^{-}$  ions in the negative-ion ESI mode [34], while individual sphingomyelins (SM) were quantified using protonated molecules  $[M+H]^{+}$  in the positive-ion ESI mode [33].

### Data analysis

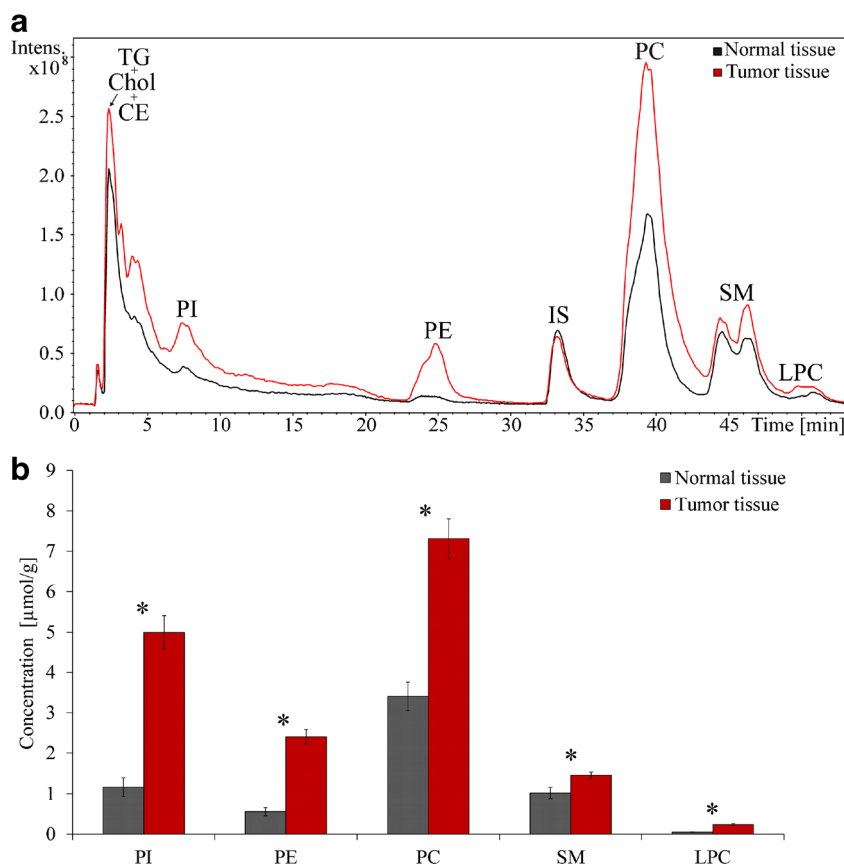
Unsupervised multivariate data analyses were performed using PCA and supervised analyses using OPLS method in the SIMCA software version 13.0 (Umetrics AB, Umeå, Sweden) [27, 30]. The Pareto scaling was used before the statistical analysis. Multivariate models were described using  $R^2$  and  $Q^2$  parameters, where  $R^2$  describes fractions of the sum of squares of all X (and Y for OPLS) that the model can explain using the latent variables, and  $Q^2$  describes fractions of the sum of squares of all X (and Y for OPLS) predicted by the model according to the cross validation or how accurately the model can be expected to predict new data. These values for all models were shown in ESM Tables S2 and S3. All statistical evaluations using PCA and OPLS method described in this work were calculated from relative abundances.

## Results and discussion

### Quantitation of individual polar lipid classes using HILIC-HPLC/ESI-MS

Total lipid extracts of normal and tumor tissues are prepared using the modified Folch method and analyzed using HILIC-HPLC/ESI-MS [33]. The breast tissue contains a large amount of nonpolar lipids, mainly TG, which results in large tailing peak containing TG and other nonpolar lipids in the HILIC chromatogram interfering significantly with other lipid classes (see ESM Fig. S1). For this reason, we perform re-extraction of total lipid extracts using hexane–methanol–water mixture to remove excessive nonpolar lipids (see ESM Fig. S1). The removal of nonpolar lipids does not change the lipidomic profiles of polar lipids. HILIC-HPLC/ESI-MS analyses of purified fractions of polar lipids show significant differences in the composition of individual lipid classes for the normal (black line) and tumor (red line) tissues of the same patient (Fig. 1a). The quantitation of individual lipid classes is performed using the previously developed validated method based on the combination of a single IS and response factors for each class related to this IS [33, 34]. This approach neglects small differences in ionization efficiencies and fragmentation behavior of individual lipids within the class similarly as the large majority of both shotgun and LC/MS lipidomic quantitations due to the lack of standards for all lipids. All lipid classes presented in Fig. 1b show statistically

**Fig. 1** **a** Positive-ion HILIC-HPLC/ESI-MS of polar lipid extracts of normal (*black line*) and tumor (*red line*) tissues of breast cancer patients. HPLC conditions: column Spherisorb Si (250×4.6 mm, 5 μm); flow rate, 1 mL/min; separation temperature, 40 °C; and gradient: 0 min, 94 % A+6 % B and 60 min, 77 % A+23 % B, where A is acetonitrile and B is 5 mM aqueous ammonium acetate. **b** Comparison of average concentrations [μmol/g] of individual lipid classes in normal and tumor tissues for ten patients with their standard errors. Peak annotation: *TG*, triacylglycerols; *Chol*, cholesterol; *CE*, cholesteryl esters; *PI*, phosphatidylinositols; *PE*, phosphatidylethanolamines; *IS*, internal standard; *PC*, phosphatidylcholines; *SM*, sphingomyelins; *LPC*, lysophosphatidylcholines. Statistically significant differences according to *T* test are indicated by an *asterisk*



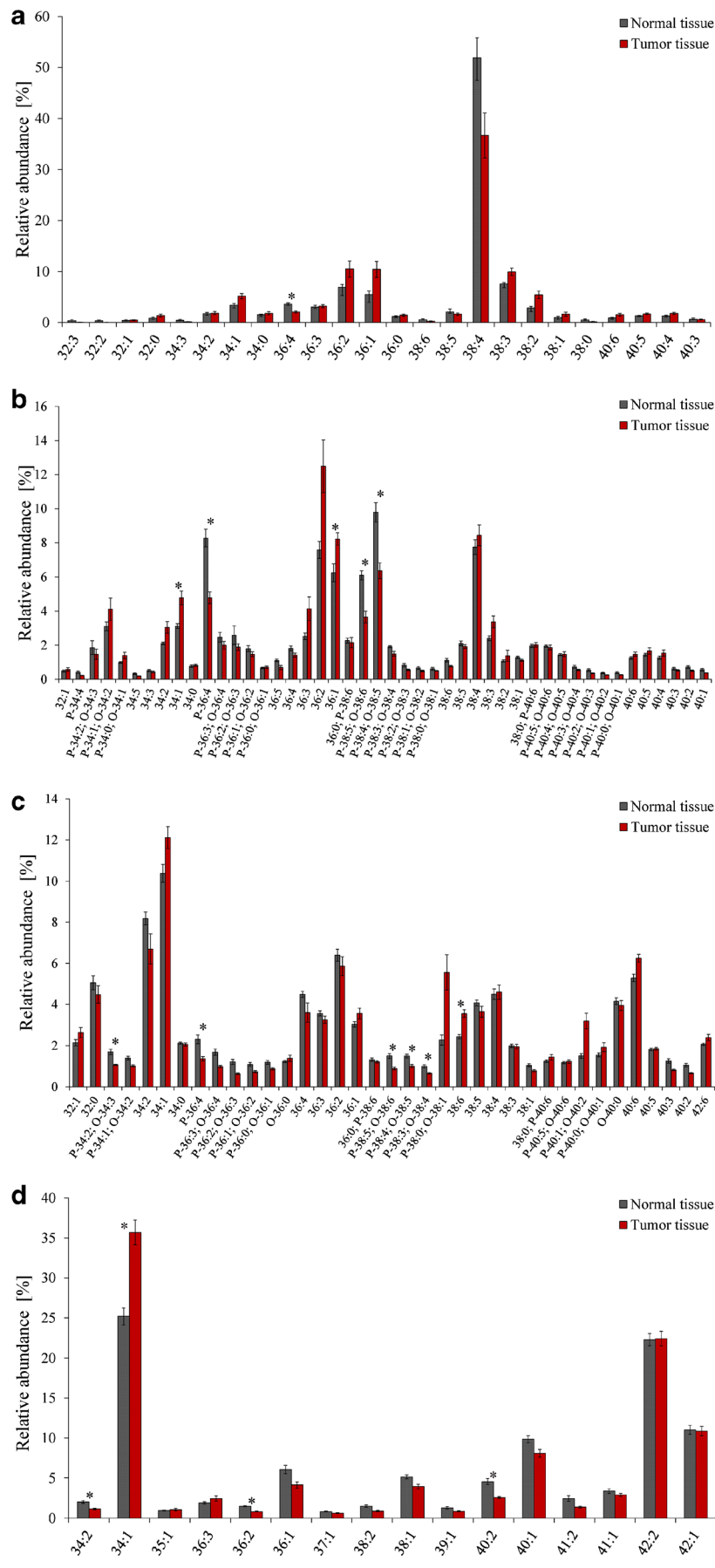
significant differences in concentrations in normal tissues (gray columns) vs. tumor tissues (red columns) of ten breast cancer patients. The reliability of differences between groups under comparison is estimated with the Holm-Bonferroni method [35]. Numerical values are displayed in ESM Table S4. Average concentrations of PI, PE, and LPC increase more than four times and for PC more than twice in tumor tissues, which show large differences in the lipid composition of normal tissues and tumor tissues. Detailed analysis of individual lipids inside lipid classes can provide important information about the lipid metabolism in the breast cancer tissue.

Analysis of individual lipid species using  $[M-H]^-$ ,  $[M-CH_3]^-$ , and  $[M+H]^+$  ions

Individual lipid species concentrations are reported by two approaches. The first approach (Fig. 2) describes relative abundances of lipid species (in %) and their proportional changes between normal and tumor tissues, which is used for MDA with a good clustering of two groups. The second one (see ESM Fig. S2) describes absolute concentrations (in μmol/g) calculated using relative abundances of individual lipids multiplied by the total concentration of the whole lipid class. Individual lipid species differ in attached fatty acyls, which are annotated by their total carbon number and double

bond number (CN:DB). Positions of individual fatty acyls on glycerol skeleton are not identified, and their shorthand notation corresponds with the established lipidomic terminology [36]. The lipid class of PI provides the greatest difference between concentrations of normal and tumor tissues (more than four times) for ten analyzed patients (Fig. 1b, ESM Table S4). Relative abundances of deprotonated molecules  $[M-H]^-$  enable to describe the composition of 24 species (Fig. 2a). The highest relative abundance in both tissues corresponds to PI 38:4 species containing two attached fatty acyls with 38 carbon atoms and 4 double bonds. The most of individual PI species has higher relative abundances in the tumor tissue except for PI 38:4 (typically PI 18:0\_20:4), PI 36:4 (PI 16:0\_20:4), and PI 38:5 (PI 18:1\_20:4). Figure 2Sb in the ESM shows concentrations in micromoles per gram for individual PI species and their differences for both tissues. Statistically significant differences according to *T* test are labeled by an asterisk (this annotation is used in all figures).

**Fig. 2** Relative abundances [%] of individual **a** PI, **b** PE, **c** PC, and **d** SM in normal and tumor tissues of ten breast cancer patients determined using relative abundances of  $[M-H]^-$  and  $[M-CH_3]^-$  ions in negative-ion mass spectra or  $[M+H]^+$  ions in positive-ion mass spectra obtained by HILIC-HPLC/ESI-MS. Statistically significant differences according to *T* test are indicated by an *asterisk*



At first, unsupervised MDA using PCA was used for individual PI species in normal and tumor tissues (see ESM Table S2; Fig. 3a). The PCA model described using two principal components shows clearly indistinguishable clusters of normal and tumor tissues. Supervised MDA using OPLS

was used for more simple understanding of individual PI species influence on clustering of these groups (see ESM Table S3; Fig. 3b). The OPLS model for individual PI species (Fig. 4) is described using 1+2+0 components, where 1 predictive component summarizes the information contained

**Fig. 3** Multivariate data analysis of relative abundances [%] of individual PI species in normal (black) and tumor (red) tissues: **a** PCA score plot, **b** OPLS score plot, and **c** OPLS S-plot

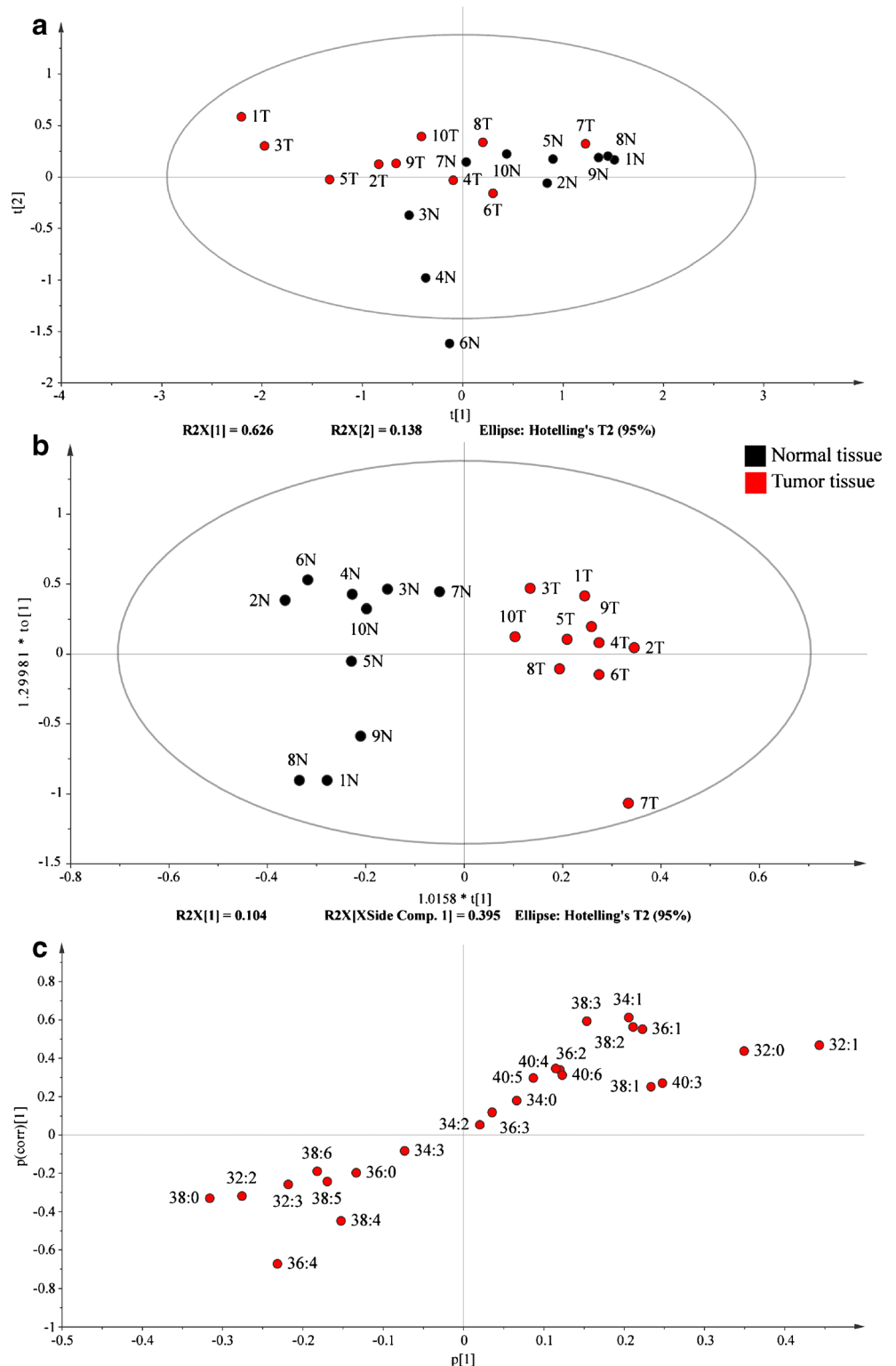
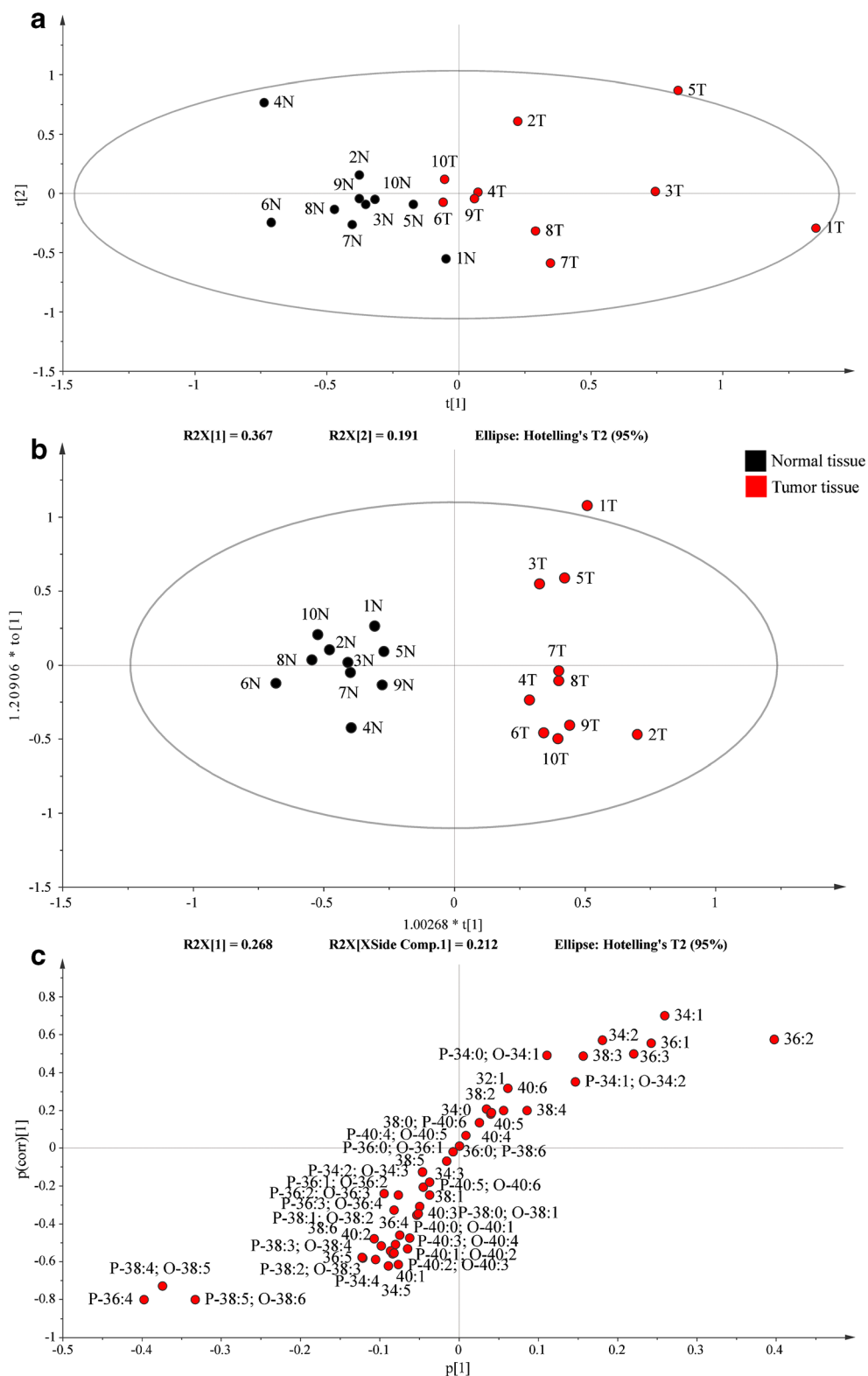


**Fig. 4** Multivariate data analysis of relative abundances [%] of individual PE species in normal (*black*) and tumor (*red*) tissues: **a** PCA score plot, **b** OPLS score plot, and **c** OPLS S-plot



in X and Y matrices, 2 orthogonal in X components expresses the information that is unique to X matrix, and 0 orthogonal in Y component expresses the information that is unique to Y matrix. The score plot (Fig. 3b) shows the clear separation of two classes (normal vs. tumor tissue) of PI species, where the

horizontal axis corresponds to the variability between classes and the vertical axis to the variability within classes. The S-plot (see ESM Fig. S3c) displays positively (PI 34:1, PI 32:1, PI 32:0) and negatively (PI 36:4, PI 38:0, PI 38:4) correlated lipids with tumor tissues. In general, the score plot is a

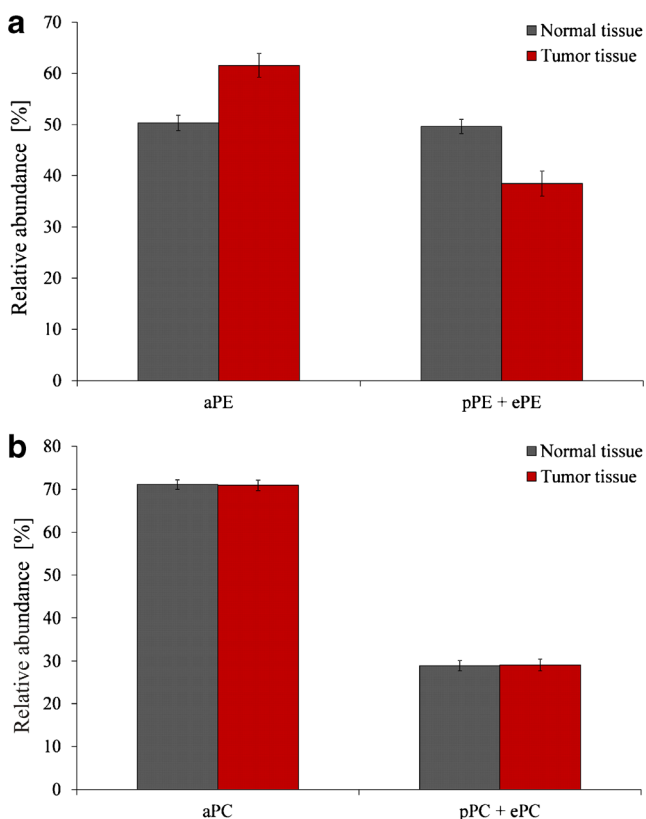


**Fig. 5** Comparison of relative abundances of **a** the sum of aPE vs. the sum of pPE+ePE species and **b** the sum of aPC vs. the sum of pPC+ePC species in normal and tumor tissues with their standard errors of ten patients

summary of the relationship between normal and tumor tissues, while the S-plot interprets patterns observed in the score plot. The S-plot (Fig. 3c) shows the effect of attached fatty acyls in PI species on the partition into classes of normal and tumor tissues. PI 36:4 (PI 16:0\_20:4), PI 38:4 (PI 18:0\_20:4), and PI 34:1 (PI 16:0\_18:1) are statistically the most reliable, where PI 36:4 and PI 38:4 are down-regulated in tumor tissues, while PI 34:1, 32:1 and 32:0 are up-regulated. On the other hand, PI species in the middle of the diagram close to the zero vertical axis (PI 34:2, PI 36:3, and PI 34:3) have a low statistical importance for the class differentiation. Obtained statistical results are comparable with Fig. 2a, but the loading plot provides a visualization of effects of individual PI on the group differentiation.

The lipid class of PE can be divided according to the type of fatty acyl linkage to the glycerol skeleton into the most commonly known group of ester-linked fatty acyls at both *sn*-1 and *sn*-2 positions (diacyls) referred as aPE, ether-linked fatty acyls in the *sn*-1 position (1-alkyl-2-acyl) referred as ethers (ePE), and vinyl ether-linked fatty acyls in the *sn*-1 position (1-alkenyl-2-acyl) referred as plasmalogens (pPE). Relative abundances and concentrations of 46 individual PE are shown in Fig. 5. Some combinations of PE (aPE, ePE, and pPE) having identical [M-H]<sup>-</sup> ions cannot be distinguished using this approach; therefore, all possible variants are reported regardless of

probably lower concentrations of ePE according to the literature [37]. The comparison of relative abundances in both tissues (Fig. 2b) describes three statistically significant PE species (P-36:4, P-38:5/O-38:6, and P-38:4/O-38:5) with higher relative abundances in normal tissues. Figure S2b in the ESM illustrates differences of individual PE concentrations in normal and tumor tissues, which are statistically significant for all PE species having higher concentrations in tumors. Unsupervised MDA of individual PE using the PCA method (Fig. 4a; see ESM Table S2) shows again that smaller clusters for normal tissues and wider clusters for tumor tissues are similar. The MDA of individual PE using the OPLS model (Fig. 4b, c) is described using 1+1+0 components (see ESM Table S3). The score plot of PE species (Fig. 4b) depicts two well-separated groups. Differences within one group are larger for tumor tissues in comparison with normal tissues possibly due to various tumor subtypes. The S-plot (Fig. 4c) shows a significant down-regulated effect of three earlier mentioned PE species in tumor tissues and, moreover, PE 34:1 (PE 16:0\_18:1) and PE 36:2 (PE 18:1\_18:1) increased in tumor tissues, which can also be correlated with the data presented in Fig. 2b.

The PC class can be also divided according to fatty acyl linkage into diacyls (aPC), ethers (ePC), and plasmalogens (pPC) similarly as for PE. Relative abundances (Fig. 2c) and concentrations (see ESM Fig. S2c) of 36 PC species illustrate five statistically significant pPC or ePC and one aPC (namely PC 38:6) species by using the comparison of relative abundances and statistically significant differences in 26 PC species by using comparison of concentrations. The PCA model (see ESM Fig. S3a and Table S2) of relative abundances of PC described using two principal components shows similar clustering as for PE. The statistical evaluation of individual PC (see ESM Fig. S3b) using the OPLS method with 1+1+0 components (see ESM Table S3) enables to obtain the information about the differentiation of normal and tumor tissues. The S-plot (see ESM Fig. S3c) describes the important effect of most pPC and ePC (especially PC containing C20:4 and saturated fatty acyl) for normal tissues and PC 40:6 (PC 22:6\_18:0), PC 38:6 (PC 22:6\_16:0), and PC 34:1 (PC 16:0\_18:1) for tumor tissues.

Plasmalogens play a critical role in cell membranes, for example in the structural function, signaling, or protection of membrane lipids against oxidation. Increased lipid oxidation associates with decreased plasmalogen levels and imbalances in lipid metabolism, which can lead to disease progression [38]. Therefore, we compare relative proportions of diacyls vs. plasmalogens and ethers in normal and tumor tissues (Fig. 5). The relative proportion of aPE in normal tissues is similar to that of pPE+ePE (50:50), but the relative proportion of aPE in tumor tissues is about one third higher than that of pPE+ePE (62:38) (Fig. 5a). Different results are obtained for the PC lipid class, where relative abundances of aPC vs. pPC+ePC are almost the same in both tissues (Fig. 5b).



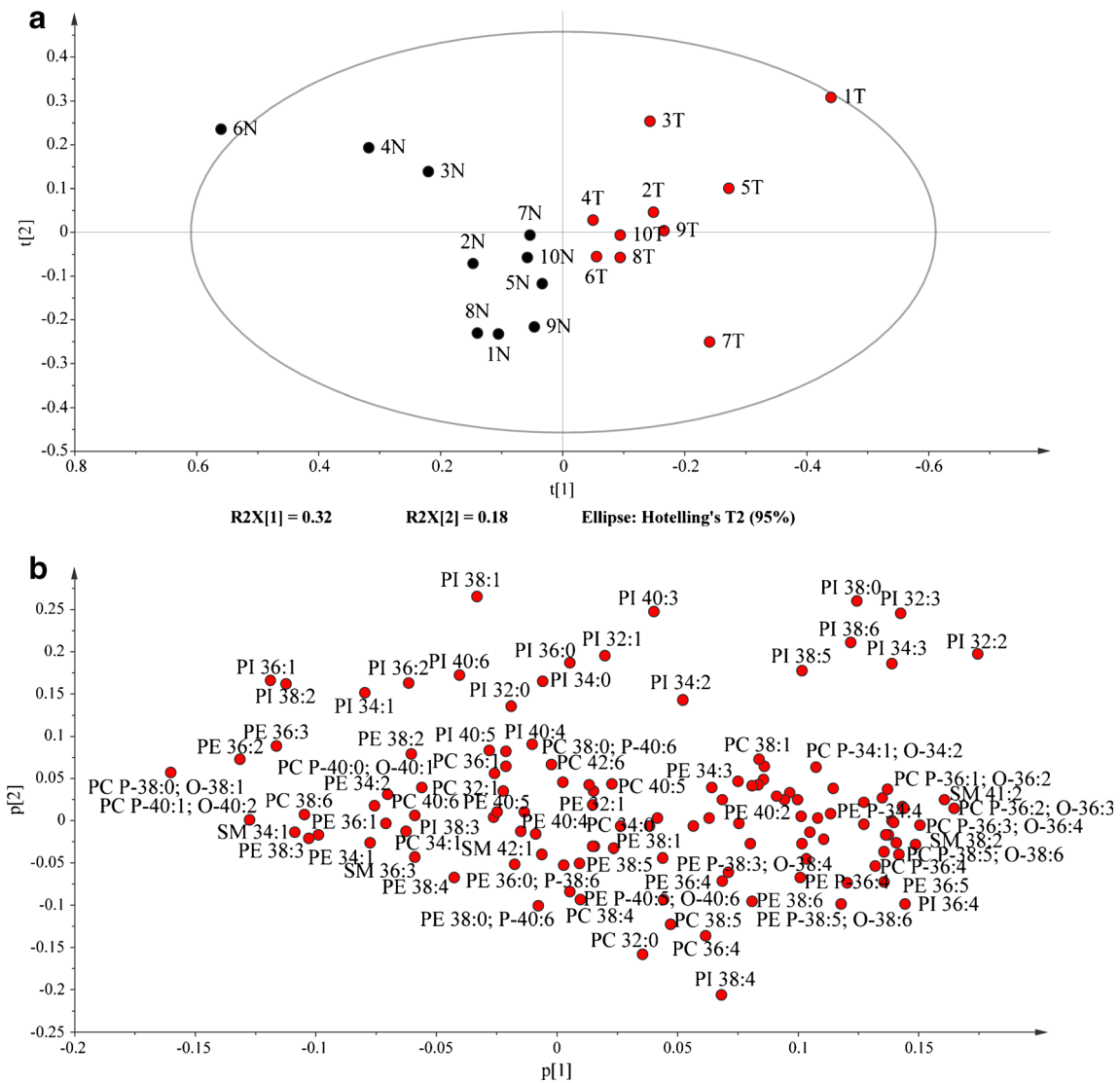


**Fig. 6** Multivariate data analysis of relative abundances of all described lipid species in normal (black circles) and tumor (red circles) tissues using unsupervised PCA method: **a** the score plot and **b** the loading plot

The SM species are analyzed using protonated molecules  $[M+H]^+$  in ESI mass spectra. This approach cannot be used for the analysis of SM 38:5 (SM 20:4\_18:1) due to the presence of sodium adduct  $[M+Na]^+$  ion of SM 36:2 with the identical nominal mass to  $[M+H]^+$  ion of SM 38:5. Relative abundances (Fig. 2d) and concentrations (see ESM Fig. S2d) of 16 individual SM species (except for SM 38:5) are compared in normal and tumor tissues. SM 34:2 (SM 16:1\_18:1), SM 34:1 (SM 16:0\_18:1), SM 36:2 (SM 18:1\_18:1), and SM 40:2 (SM 22:1\_18:1) are described as statistically significant using the comparison of relative abundances, while SM 34:1 using the comparison of concentrations. Unsupervised MDA of individual SM using the PCA model described using two principal components (see ESM Fig. S4a and Table S2) shows worse clustering of normal and tumor groups in comparison with other lipid species. The statistical evaluation using the OPLS method with 1+1+0 components (see ESM Fig. S4b, c and

Table S3) shows the most statistically reliable SM 34:1 (SM 16:0\_18:1) increasing in tumor tissues and SM 36:2 and SM 40:2 decreasing in tumor tissues (see ESM Fig. S4c). The detailed analysis of LPC cannot be performed due to low concentrations and low intensities of protonated molecules  $[M+H]^+$  in ESI mass spectra. Analysis of the total lipidome using unsupervised PCA method is shown in the score plot (Fig. 6). The loading plot (Fig. 6b) displays the relationship between X and Y matrices by using predictive components. The first component describes the separation of normal and tumor tissues—in this case, mainly PC P-38:0; O-38:1, PE 36:2, PC P-40:1; O-40:2, PI 32:2; and PC P-36:2; O-36:3. The second component shows a variability in tumor tissues, which is the most influenced by individual PI species (PI 38:1, PI 38:4). OPLS MDA of the total lipidome shows excellent results (Fig. 7a), where normal tissues form a compact group, while differences within the tumor group are larger. OPLS S-

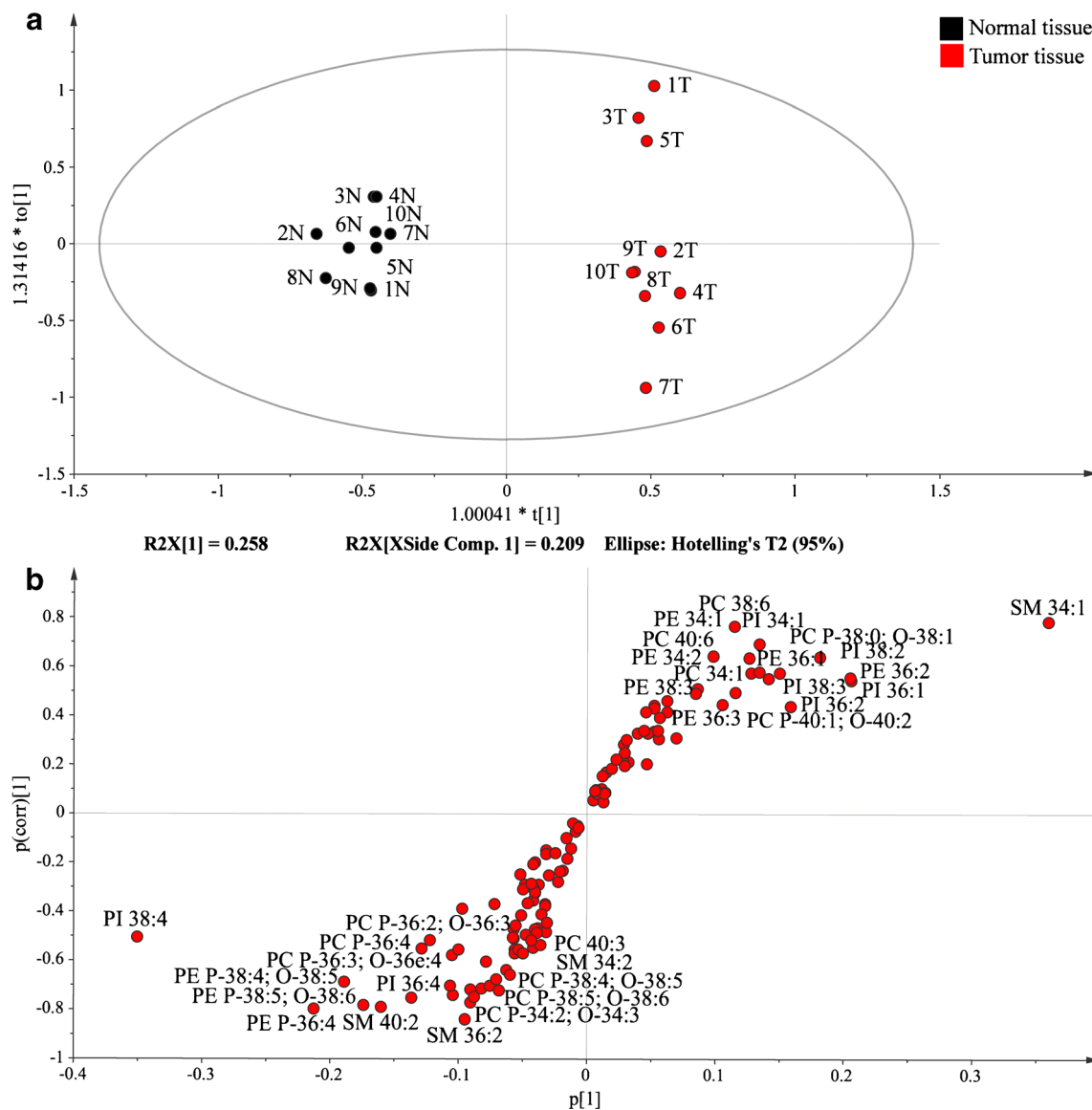


**Fig. 7** Score plot of supervised multivariate data analysis of relative abundances of all lipids in normal and tumor tissues using OPLS method: **a** score plot and **b** S-plot

plot (Fig. 7b) shows that SM 34:1 (SM d18:1/16:0) has the highest positive correlation and PE P-36:4 (PE P-20:4\_16:0) has the highest negative correlation with the tumor tissue. Both lipids exhibit high magnitude and high reliability in the OPLS model; therefore, they significantly contribute to the clustering of normal and tumor tissues.

#### Characterization of attached fatty acyls in phospholipids

The degree of lipid saturation plays an important role in de novo lipogenesis in cancer cells, because polyunsaturated fatty acyls are more susceptible to lipid peroxidation, which mediates cell death induced by oxidative stress or cytotoxic drugs [39, 40]. For this reason, we describe attached fatty acyls on the glycerol

skeleton in normal and tumor tissues by using HILIC-HPLC/ESI-MS. Table 1 shows increased relative abundances of saturated (0 DB) and low unsaturated (1–3 DB) fatty acyls and decreased level of high unsaturated (4–6 DB) fatty acyls in tumor tissues in most phospholipid classes. The biggest differences between normal and tumor tissues for saturated and low unsaturated fatty acyls are observed for pPC+ePC and pPE+ePE, while lower relative abundances in tumor tissues are detected for aPE and aPC. PI is less unsaturated in tumors. Values of average carbon number (aCN) are from 36.0 (aPC) to 40.9 (pPE+ePE), and differences between normal and tumor groups are relatively small. Average double bond (aDB) number varies from 2.0 (pPC+ePE) to 3.8 (pPE+ePE) for phospholipid classes,

**Table 1** Relative abundances [%] of saturated (0 DB), low unsaturated (1–3 DB), and high unsaturated (4–6 DB) fatty acyls on the glycerol skeleton in normal and tumor tissues, their average carbon number (aCN), and average double bond (aDB) number

Lipid class	Saturated (0 DB)		Low unsaturated (1–3 DB)		High unsaturated (4–6 DB)		aCN		aDB	
	Normal	Tumor	Normal	Tumor	Normal	Tumor	Normal	Tumor	Normal	Tumor
PI	4.1	4.8	34.2	49.5	61.7	45.7	37.3	37.1	3.2	2.8
PE	6.3	6.5	42.6	52.2	51.1	41.3	38.6	38.4	3.3	3.0
aPE	9.1	7.6	53.5	61.8	37.4	30.6	36.8	36.6	2.6	2.4
pPE+ePE	10.8	13.8	30.7	34.2	58.5	52.0	40.2	40.9	3.8	3.7
PC	17.0	19.3	50.6	50.9	32.4	29.9	37.4	37.6	2.6	2.5
aPC	11.0	10.3	56.4	55.6	32.6	34.1	36	36	2.5	2.6
pPC+ePC	28.3	35.0	39.8	42.6	31.9	22.5	37.6	38.1	2.5	2.0
SM	0	0	100	100	0	0	38.5	38	1.4	1.3
Average <sup>a</sup>	12.4	13.9	44.0	49.5	43.7	36.6	37.7	37.8	2.9	2.7

<sup>a</sup> Average parameters of phospholipids (excluding SM) obtained by averaging each column, i.e., average of values for PI, PE, aPE, pPE+ePE, PC, aPC, and pPC+ePC

and values of aDB are lower for tumor tissues in all lipid classes, except for aPC. The class of SM contains mainly monounsaturated attached fatty acyls, and all SM belong to low unsaturated fatty acyls. The described behavior of saturated, low unsaturated, and high unsaturated fatty acyls in tumor tissues is in agreement with that in the literature, but the present methodology provides tools for reliable quantitation and generalization of these trends for both class concentrations and individual lipid species as well.

## Conclusions

The statistically significant increase of concentrations observed for several phospholipid classes and also lipid species within these classes is detected in breast tumor tissues of ten patients compared to surrounding normal tissues of the same patients. The decrease of relative abundances is observed for pPE and ePE (but not for pPC and ePC), which may be related to combined reasons not specific only to cancer, such as the oxidative stress and inflammation as side effects that accompany the tumor growth. The presence of phospholipids with the general formula C34:1 (mainly combination of C16:0 and C18:1) has shown marked association with tumor tissues for several lipid classes, while similar but less pronounced trend can be found for other phospholipids with low saturation level. The present study demonstrates a proof-of-concept of applicability of developed analytical methodology, but it also has certain limitations due to its pilot nature. All patients in this study are classified as luminal A or luminal B breast cancer, and less frequent subtypes, including hormone receptor-negative, HER-2 positive, and triple negative tumors, are not represented in this pilot cohort. The possible association between breast cancer subtype and phospholipid composition could be reliably addressed in future larger cohort of patients.

**Acknowledgments** This work was supported by ERC CZ project No. LL1302 sponsored by the Ministry of Education, Youth and Sports of the Czech Republic. E.C. acknowledges the support of the grant project no. CZ.1.07/2.3.00/30.0021 sponsored by the Ministry of Education, Youth and Sports of the Czech Republic. The help of Blanka Červená and Vitaliy Chagovets (University of Pardubice) in the extraction and data analysis and Martin Hill (Institute of Endocrinology) in the statistical evaluation is acknowledged.

## References

1. Pelengaris S, Khan M (2013) Wiley: Oxford
2. Rosen L, Rosen G (2013) <http://cancer.org/>: Atlanta
3. Thomson CA, Thompson PA (2009) *Future Oncol* 5:1257–1269
4. Azordegan N, Fraser V, Le K, Hillyer LM, Ma DWL, Fischer G, Moghadasian MH (2013) *Mol Cell Biochem* 374:223–232

5. Pender-Cudlip MC, Krag KJ, Martini D, Yu J, Guidi A, Skinner SS, Zhang Y, Qu XY, He CW, Xu Y, Qian SY, Kang JX (2013) *Cancer Sci* 104:760–764
6. Lv WW, Yang TS (2012) *Clin Biochem* 45:127–133
7. Shannon J, King IB, Moshofsky R, Lampe JW, Gao DL, Ray RM, Thomas DB (2007) *Am J Clin Nutr* 85:1090–1097
8. Kang JX, Liu A (2013) *Cancer Met Rev* 32:201–210
9. Corsetto PA, Montorfano G, Zava S, Jovenitti IE, Cremona A, Berra B, Rizzo AM (2011) *Lipids Health Dis*. 10
10. Spencer L, Mann C, Metcalfe M, Webb M, Pollard C, Spencer D, Berry D, Steward W, Dennison A (2009) *Eur J Cancer* 45:2077–2086
11. Doria ML, Cotrim CZ, Simoes C, Macedo B, Domingues P, Domingues MR, Helguero LA (2013) *J Cell Physiol* 228:457–468
12. Doria ML, Cotrim Z, Macedo B, Simoes C, Domingues P, Helguero L, Domingues MR (2012) *Breast Cancer Res Tr* 133:635–648
13. Hua X, Zhou ZX, Yuan L, Liu SQ (2013) *Anal Chim Acta* 788:135–140
14. Chughtai K, Jiang L, Greenwood TR, Glunde K, Heeren RMA (2013) *J Lipid Res* 54:333–344
15. Hilvo M, Denkert C, Lehtinen L, Muller B, Brockmoller S, Seppanen-Laakso T, Budczies J, Bucher E, Yetukuri L, Castillo S, Berg E, Nygren H, Sysi-Aho M, Griffin JL, Fiehn O, Loibl S, Richter-Ehrenstein C, Radke C, Hyotylainen T, Kallioniemi O, Iljin K, Oresic M (2011) *Cancer Res* 71:3236–3245
16. Smith RE, Lespi P, Di Luca M, Bustos C, Marra FA, de Alaniz MJT, Marra CA (2008) *Lipids* 43:79–89
17. Hammad LA, Wu GX, Saleh MM, Klouckova I, Dobrolecki LE, Hickey RJ, Schnaper L, Novotny MV, Mechref Y (2009) *Rapid Commun Mass Spectrom* 23:863–876
18. Kim H, Min HK, Kong G, Moon MH (2009) *Anal Bioanal Chem* 393:1649–1656
19. Holčápek M, Jirásko R, Lísá MJ (2012) *Chromatogr A* 1259:3–15
20. Han XL, Yang K, Gross RW (2012) *Mass Spectrom Rev* 31:134–178
21. Yang K, Han X (2011) *Metabolites* 1:21–40
22. Begley JKP, Redpath TW, Bolan PJ, Gilbert FJ (2012) *Breast Cancer Res*. 14
23. Glunde K, Jie C, Bhujwala ZM (2004) *Cancer Res* 64:4270–4276
24. Klomp DWJ, van de Bank BL, Raaijmakers A, Korteweg MA, Possanzini C, Boer VO, de Berg C, van de Bosch M, Luijten PR (2011) *NMR Biomed* 24:1337–1342
25. Merchant TE, Meneses P, Gierke LW, Denotter W, Glonek T (1991) *Br J Cancer* 63:693–698
26. Kirwan GM, Johansson E, Kleemann R, Verheij ER, Wheelock AM, Goto S, Trygg J, Wheelock CE (2012) *Anal Chem* 84:7064–7071
27. Eriksson L, Byrne T, Johansson E, Trygg J, Vikström C (2013) *Multi- and megavariate data analysis. Basic principles and applications. Third revised edition.* MKS Umetrics AB, Malmö
28. Wold S, Sjostrom M, Eriksson L (2001) *Chemom Intell Lab Syst* 58: 109–130
29. Trygg J, Wold S (2002) *J Chemom* 16:119–128
30. Trygg J (2002) *J Chemom* 16:283–293
31. Folch J, Lees M, Stanley GHS (1957) *Biol Chem* 226:497–509
32. Lísá M, Cífková E, Holčápek MJ (2011) *Chromatogr A* 1218:5146–5156
33. Cífková E, Holčápek M, Lísá M, Ovčáčíková M, Lyčka A, Lynen F, Sandra P (2012) *Anal Chem* 84:10064–10070
34. Cífková E, Holčápek M, Lísá M (2013) *Lipids* 48:915–928
35. Holm S (1979) *Scand J Stat* 6:65–70
36. Liebisch G, Vizcaino JA, Kofeler H, Trotzmuller M, Griffiths WJ, Schmitz G, Spener F, Wakelam MJO (2013) *Lipid Res* 54:1523–1530
37. Nagan N, Zoeller RA (2001) *Prog Lipid Res* 40:199
38. Bravenman NE, Moser AB (2012) *Biochim Biophys Acta-Mol Basis Dis* 1822:1442–1452
39. Rysman E, Brusselmans K, Scheys K, Timmermans L, Derua R, Munck S, Van Veldhoven PP, Waltregny D, Daniels VW, Machiels J, Vanderhoydonc F, Smans K, Waelkens E, Verhoeven G, Swinnen JV (2010) *Cancer Res* 70:8117–8126
40. Santos CR, Schulze A (2012) *Febs J* 279:2610–2623